THE JOURNAL OF BIOLOGICAL CHEMISTRY VOL. 285, NO. 23, pp. 17918–17929, June 4, 2010

Molecular Characterization of Mutant *Arabidopsis* Plants with Reduced Plasma Membrane Proton Pump Activity*[S]

Received for publication, January 8, 2010, and in revised form, March 15, 2010 Published, JBC Papers in Press, March 26, 2010, DOI 10.1074/jbc.M110.101733

Miyoshi Haruta[‡], Heather L. Burch[‡], Rachel B. Nelson[§], Greg Barrett-Wilt[‡], Kelli G. Kline[‡], Sheher B. Mohsin[¶], Jeffery C. Young[‡1], Marisa S. Otegui[‖], and Michael R. Sussman[‡§2]

From the [‡]Biotechnology Center, Departments of [§]Biochemistry and [‖]Botany, University of Wisconsin, Madison, Wisconsin 53706 and [¶]Agilent Technologies Inc., Schaumburg, Illinois 60173

Arabidopsis **mutants containing gene disruptions in *AHA1* and *AHA2*, the two most highly expressed isoforms of the *Arabidopsis* plasma membrane H$^+$-ATPase family, have been isolated and characterized. Plants containing homozygous loss-of-function mutations in either gene grew normally under laboratory conditions. Transcriptome and mass spectrometric measurements demonstrate that lack of lethality in the single gene mutations is not associated with compensation by increases in RNA or protein levels. Selected reaction monitoring using synthetic heavy isotope-labeled C-terminal tryptic peptides as spiked standards with a triple quadrupole mass spectrometer revealed increased levels of phosphorylation of a regulatory threonine residue in both isoforms in the mutants. Using an extracellular pH assay as a measure of *in vivo* ATPase activity in roots, less proton secreting activity was found in the *aha2* mutant. Among 100 different growth conditions, those that decrease the membrane potential (high external potassium) or pH gradient (high external pH) caused a reduction in growth of the *aha2* mutant compared with wild type. Despite the normal appearance of single mutants under ideal laboratory growth conditions, embryos containing homozygous double mutations are lethal, demonstrating that, as expected, this protein is absolutely essential for plant cell function. In conclusion, our results demonstrate that the two genes together perform an essential function and that the effects of their single mutations are mostly masked by overlapping patterns of expression and redundant function as well as by compensation at the post-translational level.**

In animals, the sodium pump is the primary active transport system and creates a membrane potential and sodium gradient that are used by all ion channels and cotransporters (1, 2). In higher plants and fungi, however, the transport of all solutes across the plasma membrane is coupled to a proton gradient rather than a sodium gradient. Thus, in these organisms, a plasma membrane proton pump creates a protonmotive force at the plasma membrane that drives all channels and cotransporters. Given the known importance of transport at the plasma membrane for life functions, it is not surprising that genetic studies of the sodium pump in nematodes, fruit flies, zebrafish, and mice, as well as with the proton pump of yeast, all conclusively demonstrate the lethal effects of loss-of-function mutations for a gene encoding the primary active transporter (Table 1) (3–11). In contrast, although there have been several reports of altered growth of mutant plants containing genetic alterations in the plasma membrane proton pump (12–17), none of these studies have provided evidence indicating that this enzyme performs an essential function for plant life. In this study, we present evidence clearly demonstrating that the plasma membrane proton pump is essential for plant growth. We show that *AHA1* and *AHA2* (for *Arabidopsis* H$^+$-ATPase isoforms 1 and 2), the two most highly expressed members of the *AHA* gene family, perform overlapping functions that mask the lethality in single gene loss-of-function mutants. We also describe phenotypic screening that supports the *in planta* role of the proton pump in generating a protonmotive force and mass spectrometric methods that allow a more detailed and quantitative analysis of the *in vivo* regulation of these proteins at the post-translational level.

EXPERIMENTAL PROCEDURES

Plant Materials and Growth Conditions—Mutants (ecotype Columbia) carrying T-DNA insertions in *AHA1* (*aha1–6*, SALK016325; *aha1–7*, SALK065288; and *aha1–8*, SALK118350) and *AHA2* (*aha2–4*, SALK082786, and *aha2–5*, SALK022010) were obtained from the Arabidopsis Biological Resource Center (Ohio State University) (18). Seeds were germinated on plates containing half-strength M&S[3] salts, 1% (w/v) sucrose, and 0.7% (w/v) agar. Plants that were transferred to soil/perlite mixture (Jiffy-Mix, Jiffy Products of America, Lorrain, OH; horticultural perlite, The Schundler Co., Metuchen, NJ) were grown at 21 °C under constant light or 22 °C with a regime of 16 h of light/8 h of dark.

T-DNA Mutant Identification and Plant Genotyping—Plant genomic DNA was extracted using the method of Krysan *et al.* (19), with the elimination of the phenol/chloroform extraction step. The location of the T-DNA insertion in *AHA1* or *AHA2* was determined by sequencing PCR fragments containing the

* This work was supported by grants from the Department of Energy and the National Science Foundation (to M. R. S.) and by National Science Foundation Grant MCB-0619736 (to M. S. O.).

[S] The on-line version of this article (available at http://www.jbc.org) contains supplemental sequences and additional references.

[1] Present address: Dept. of Biology, Western Washington University, Bellingham, WA 98225.

[2] To whom correspondence should be addressed: 425 Henry Mall, Madison, WI 53706. Tel.: 608-262-8608; Fax: 608-262-6748; E-mail: msussman@wisc.edu.

[3] The abbreviations used are: M&S, Murashige and Skoog; MS, mass spectrometry; HPLC, high pressure liquid chromatography; RT, reverse transcription; WT, wild type; GUS, β-glucuronidase.

TABLE 1
Loss-of-function mutations of plasma membrane P-type ATPase pump maintaining electrochemical gradients cause lethality in many eukaryotic model organisms

Organisms	Mutagen	Gene	Terminal phenotype	Refs.
Yeast	Homologous recombination	*PMA1* (H^+ pump)	Haploid cell lethality	3
Thale cress	T-DNA insertion	*AHA1 AHA2* double	Embryonic lethality	This study
		AHA3 (H^+ pump)	Male gamete lethality	4
Nematode	Ethyl methane sulfonate	*eat-6* (Na^+/K^+ pump α)	Lethality at a larval stage	5
Fruit fly	P-element insertion	$ATPalpha^{2206}$	Embryonic lethality	6
	Ethyl methane sulfonate	$ATP\alpha^{H64}$ (Na^+/K^+ pump α)		7
Zebrafish	*N*-ethyl *N*-nitrosourea	$atp1a1a\alpha^{m883}$	Embryonic lethality	8
	Spontaneous	*had* (Na^+/K^+ pump α1B1)		9
Mouse	Homologous recombination	*Na K-ATPase* α*2,* α3(Na^+/K^+ pump α)	Lethality at embryo and infant	10

junction of the T-DNA and plant genomic DNA. The genotypes of plants were determined by PCR with allele-specific primers. The sequences of the PCR primers are provided in the supplemental material.

RNA Extraction, Quantitative RT-PCR, and Microarray Analyses—RNA was extracted from 1-week-old seedlings with the Plant RNeasy kit (Qiagen). For transcriptional profiling with GeneChip *Arabidopsis* ATH1 Genome Array (Affymetrix), RNA was processed using standard protocols at the Gene Expression Center, University of Wisconsin, Madison. Transcriptome data were normalized and analyzed with the Affymetrix GeneChip operating software and the Robust Multichip Average (RMA) method (20). For quantitative RT-PCR, total RNA was extracted from 10-day-old seedlings, reverse-transcribed (Invitrogen), and subjected to PCR using the iCycler real time PCR system (Bio-Rad) with SYBR Premix (Takara). Sequences of primers used for quantitative RT-PCR are provided in the supplemental material.

Plasma Membrane Preparation—*Arabidopsis* seedlings were grown in half-strength M&S liquid media as described previously (21). Two-week-old seedlings (20 g) were extracted with 50 ml of buffer (300 mM sucrose, 100 mM Tris-HCl, pH 7.6, 25 mM EDTA-Na_2, 25 mM NaF, 1 mM Na_2MoO_4, 0.5% (w/v) polyvinylpyrrolidone, 1 mM phenylmethylsulfonyl fluoride, 1 μg/ml pepstatin, 1 μg/ml E-64, 1 μM bestatin, 100 μM 1,10-phenanthroline, and 1 mM dithiothreitol), filtered through two layers of Miracloth, and spun 80,000 $\times$ *g* for 50 min at 4 °C. The pellet was resuspended in 9 ml of suspension buffer (300 mM sucrose, 10 mM Tris-HCl, pH 7.5, and 1 mM EDTA-Na_2) and subjected to two-phase separation to enrich the plasma membrane fraction (22). The upper layer was spun at 80,000 $\times$ *g* for 50 min at 4 °C, and the pellet was resuspended in 2 ml of suspension buffer. Protein concentration was determined by the BCA assay (Pierce).

AHA Peptide Quantitation via Mass Spectrometry—Aliquots of 200 μl, corresponding to ~120 μg of total protein from each plasma membrane preparation, were precipitated with chloroform/methanol/water. Pellets were washed twice with 80% acetone and resolubilized in 7.2 M urea and 1× PhosStop (Roche Applied Science) in 45 mM ammonium bicarbonate, pH 8. Urea was then diluted to a final concentration of 1 M with 45 mM ammonium bicarbonate, including 1× PhosStop. Solubilized proteins were reduced with 2 mM dithiothreitol and alkylated with 5 mM iodoacetamide. The alkylation reaction was quenched by further addition of dithiothreitol to 2 mM and trypsin (Promega) was added at an *E*:S ratio of 1:20 (6 μg). Digestion was quenched after 16 h by the addition of neat trifluoroacetic acid to reduce the pH to ~2. Samples were desalted and concentrated by C18 solid phase extraction using SPEC tips (Varian) with a capacity of 200 μg. Peptides were eluted with 80% (v/v) acetonitrile, 0.5% (v/v) acetic acid in water. Acetonitrile was removed by vacuum centrifugation, and peptides were reconstituted in 60 μl of 0.5% (v/v) acetic acid in water (2 μg/μl). Digests were analyzed by liquid chromatography/MS on an LTQ-Orbitrap hybrid mass spectrometer (ThermoFisher Scientific). HPLC was performed using an Agilent 1100 HPLC system consisting of an isocratic pump for sample loading onto an Agilent Zorbax C_{18} trapping column (0.3 $\times$ 5 mm, 5-μm particles) and a nanopump for elution from the trapping column and onto an in-house built analytical column fabricated from 360 μm outer diameter $\times$ 75 μm inner diameter fused silica packed to a length of 15 cm with 3 μm of Magic C18 (Michrom) with an integrated electrospray emitter tip pulled to a diameter of ~2 μm. Peptides were gradient-eluted using a water/acetonitrile binary solvent system, in which solvent A was 0.1 M acetic acid in water and solvent B was 0.1 M acetic acid, 95% acetonitrile (v/v) in water. Sample loading and desalting were performed over 20 min at a flow rate of 15 μl/min using the isocratic HPLC pump to deliver 0.1 M acetic acid, 1% acetonitrile. Following sample loading, elution was performed at 200 nl/min by increasing solvent B from 1 to 40% over 195 min, 40 to 60% over 20 min, and 60 to 100% over 5 min, after which the stationary phases were re-equilibrated at the initial conditions for 30 min. The LTQ-Orbitrap mass spectrometer was operated in data-dependent mode for automated simultaneous acquisition of MS survey spectra and MS/MS spectra. MS survey spectra were acquired at 100,000 resolving power over the *m*/*z* range 300–2000 in the Orbitrap with external mass calibration. MS/MS spectra were performed on the five highest abundance signals present in the survey scan, requiring that they be present in the 2+ or higher charge state and that they pass the dynamic exclusion criteria. Post-acquisition data analysis consisted of data base searching using Mascot 2.2 (Matrix Science) and a data base composed of TAIR release 9 (downloaded on June 19, 2009) to which were added common contaminant proteins such as trypsin and human keratins. The peptides identified by data base searching were imported into Scaffold 2 (Proteome Software), which was used to identify detected peptides with unique sequences to discriminate between the various AHA isoforms. Two such peptides were used to assess abundance of AHA1 and AHA2 among the three genotypes analyzed. These peptides arise from

amino acids 407 to 420 (AHA1, $^{+}$TALTYIDSDGNWHR^{-}; AHA2, $^{+}$TALTYIDGSGNWHR^{-}) and amino acids 471 to 490 (AHA1, $^{+}$ESPGGPWEFVGLLPLFDPPR^{-}; AHA2, $^{+}$ESPGAPWEFVGLLPLFDPPR^{-}). AHA1 and AHA2 protein abundance was determined by calculating the area of extracted ion chromatograms of the isoform-specific peptides from the different plants using the Xcalibur Qual Browser software (ThermoFisher Scientific). A total of four replicate analyses was performed for each genotype.

Selective Reaction Monitoring Mass Spectrometry Analysis—Total proteins from enriched plasma membrane samples (wild type, *aha1–6*, *aha2–4*) were isolated from the supernatant using a methanol/chloroform/water extraction as described previously (23). Precipitated proteins were solubilized in 8 M urea containing phosphatase inhibitor mixture (1× PhosStop, Roche Applied Science). Samples were diluted to 1 M urea, and a BCA protein assay was performed to determine protein concentration. Samples were then diluted to contain 1 mg/ml total protein concentration. Disulfide bonds were reduced using dithiothreitol (5 mM, 30 min), alkylated with iodoacetamide (15 mM, 30 min), and protein-digested using trypsin (1:100 trypsin to protein ratio, 37 °C, overnight). Resulting peptide samples were acidified (0.1% trifluoroacetic acid) and concentrated using a solid phase extraction procedure (C18 SepPak, Waters).

Trypsin-digested plasma membrane samples were utilized for creating standard calibration curves for each of the four peptides of interest: AHA1 Thr-948, AHA1 pThr-948, AHA2 Thr-947, and AHA2 pThr-947. Isotope-labeled leucine (^{13}C) peptides were synthesized for each peptide of interest and added to each of the biological samples so that the final concentration of the labeled peptides was 100 amol to 100 fmol per μl. Samples were loaded (2 μg) onto the Agilent Phospho-CHiP. The Agilent Phospho-CHiP consisted of a TiO_2 enrichment column sandwiched between two reverse phase C18 columns. This allowed both phosphorylated peptides and nonphosphorylated peptides to be trapped and eluted separately. Trapping, enrichment, and analysis were performed on an Agilent 1200 HPLC system, consisting of a loading capillary pump operating at 4 μl/min flow and a nanoflow pump operating at 300 nl/min. Peptides were trapped at 4 μl/min using 100% solvent A (0.6% acetic acid and 2% formic acid in 2% acetonitrile). The sample was retained on the first reverse phase C18 enrichment column. After switching the enrichment columns in line, all peptides were eluted off the first C18 enrichment column by gradient elution. All peptides were then eluted off the first C18 enrichment column by gradient elution. Phosphorylated peptides bound to the TiO_2 section, whereas all other peptides with no TiO_2 affinity were transferred to the C18 separation column. Analysis was performed subsequently with a nanoflow analytical pump gradient from 5 to 70% solvent B (100% acetonitrile, 0.6% acetic acid, 0.5% formic acid) over 40 min at 300 nl/min. Elution of phosphorylated peptides from the TiO_2 section to the C18 section was then achieved by injection of 15 μl of elution buffer, pH 9.0 (Phospho-CHiP-Kit, Agilent Technologies). Analysis of the eluted (phosphorylated) peptides was performed by switching the precolumn to be in line with the analytical column for a second H_2O/acetonitrile gradient. Immediately afterward, an injection of 4 μl of regeneration solution (Phospho-CHiP kit, Agilent Technologies) was performed to wash and re-equilibrate the TiO_2 precolumn.

Doubly charged parent ions and at least three to four singly charged fragment y-ions from each of the four peptides of interest were monitored using selective reaction monitoring on the Agilent 6460-QQQ. All data were acquired with a Q1 resolution of 0.7 atomic mass unit and Q3 resolution of 1.2 atomic mass units with each transition monitored with a dwell time of 20 ms. The *RF*-only q2 collision cell was pressurized with nitrogen gas. All plasma membrane samples were analyzed a minimum of three times with isotope-labeled internal standard added from 100 amol to 100 fmol levels in each analysis.

Peptide responses of both the endogenous peptides and the isotope-labeled internal standards were determined by the area under the curve of the total ion current. Calibration curves were produced by plotting the ion intensity of the isotope-labeled internal standard peptide *versus* the amount of synthetic standard present, and endogenous peptide levels were determined by comparison with the standard calibration curve. Average concentrations were calculated across technical replicates and standard deviations produced. Coefficients of variance were calculated by taking the ratio of the standard deviation of peptide signal over the technical replicates to the average of the peptide concentration. Coefficients of variance are represented as percentages. Statistically significant differences in peptide levels were determined using a two-tailed Student's *t* test assuming unequal variance.

Microscopy and Staining—To visualize the frequency of aborted seed development, fully elongated green siliques of wild type or mutant plants were harvested, manually opened, and viewed using a Nikon SMZ1500 stereomicroscope. Images were captured using a Spot Insight color digital camera (Diagnostic Instruments, Inc.). Developing seeds from *aha1–6/aha1–6;AHA2/aha2–4* and *AHA1/aha1–6;aha2–4/aha2–4* plants were fixed in 2% glutaraldehyde, dehydrated in ethanol series, and embedded in LR White. Sections were stained with 1% toluidine Blue.

β-Glucuronidase (GUS) Reporter Assay—A 3.5-kb DNA fragment containing the *AHA1* promoter region and the first exon (14 amino acids) was PCR-amplified and cloned into pCAMBIA1301 at the EcoRI and NcoI sites to generate an *AHA1* promoter-GUS fusion construct. Plants carrying this transcriptional reporter were generated via *Agrobacterium*-mediated transformation (strain GV3101) described in Ref. 24. Multiple transgenic plants were subjected to GUS immunoblotting to verify the production of GUS protein. T2 plants homozygous for a single insertion of the transgene were selected and used for GUS assay. Siliques of various developmental stages were harvested and incubated at 37 °C for 16 h in the following reaction mixture: 50 mM sodium phosphate buffer, pH 7.2, 0.2% Triton X-100, 2 mM potassium ferrocyanide, 2 mM potassium ferricyanide, 15% methanol, and 2 mM 5-bromo-4-chloro-3-indolyl-β-D-glucuronic acid. The stained tissues were subjected to washing with a series of ethanol concentrations, fixation, embedding, and sectioning.

Molecular Complementation—A 9.9-kb genomic DNA fragment containing the *AHA1* promoter region (3377 bp), *AHA1*, and 1100 bp downstream from the stop codon was amplified by

PCR from BAC clone F19F24 (the *Arabidopsis* Biological Resource Center), using the following primers: 5′-GCCCTCGCTATATTGATGTCAG-3′ and 5′-CTTTGGACGTGACTCGCAGA-3′. The PCR fragment was first cloned into the pCR2.1 vector with TA cloning (Invitrogen) and then subcloned into the pCAMBIA1200 binary vector, which confers hygromycin resistance as the plant selection marker, at the SalI and SacI restriction sites. The resulting plasmid was used to introduce into *aha1–6/aha1–6;AHA2/aha2–4* plants as describe above. Transgenic seedlings were selected on M&S plates containing 25 μg/ml hygromycin. Hyg^R *aha1–6; aha2–4* homozygous double mutant plants whose embryonic lethality was complemented by the presence of an *AHA1* transgene were identified using PCR with locus-specific primers. Primers used to identify the endogenous *AHA1* allele were 5′-CGACGAATGATCTAATCACAAGC-3′ and 5′-CAAAGTCCGGTTAAGGGTATTTC-3′, and those used to identify the *AHA1* transgene were 5′-TGTAAAACGACGGCCAGTG-3′ and 5′-TCATGTGATTTCTTGCCATC-3′. For complementation with the *AHA2* transgene, a 10-kb genomic DNA fragment containing the *AHA2* promoter region (4337 bp), *AHA2*, and 586-bp downstream from the stop codon was obtained by PmlI-digesting BAC clone F9N11. The resulting DNA fragment was cloned into pCR2.1 at the EcoRV site and again subcloned into the pCAMBIA1200 at the SalI and SacI sites. The resulting plasmid was introduced into *AHA1/aha1–6;aha2–4/aha2–4* plants as described previously. Complemented plants were identified as described above. Primers used to identify the *AHA2* transgene were 5′-CATGTTGGCAAGCTGCTC-3′ and 5′-AAATTAGCAGGCGCATGT-3′.

Site-directed Mutagenesis—A restriction enzyme site XbaI was introduced to AHA2 via the QuikChange II XL system (Stratagene) using the following pair of primers: 5′-CGGTTTACGCCAATCTAGAGGAATTTGCAAAG-3′ and 5′-CTTTGCAAATTCCTCTAGATTGGCGTAAACCG-3′. This insertion resulted in a mutation at the Trp-807 to Leu-Glu. Into the XbaI site, green fluorescent protein gene was inserted to create putative an AHA2-GFP translational fusion protein with a molecular mass, ~125 kDa. The AHA2-GFP fusion construct was transformed to the mutant plants via *Agrobacterium* as described above.

Root Growth Phenotyping—Seeds were germinated on vertically positioned half-strength M&S plates for 3 days. Seedlings were transferred to the media supplemented with additives and grown for 4 days. During the entire course of experiments, seedlings were grown under continuous light (25 $\mu mol\ m^{-2}\ s^{-1}$). Root growth was quantified with the ImageJ software (www.nih.gov). Root growth results shown in Fig. 4 are one representative of triplicate analyses with each containing 14 seedlings. Growth conditions used for screening root phenotypes are provided in the supplemental material.

Extracellular Acidification Assay—A five-day-old single seedling were incubated in 250 μl of ¼ strength M&S media (pH 6.2, unbuffered), including 1% sucrose and 30 μg/ml fluorescein isothiocyanate/dextran (M_r 10,000, Sigma) for 16 h. Fluorescent emission was detected at 535 nm with excitation at 485 nm, using a microplate reader (Tecan SpectraFluor Plus). Media pH were calibrated by a standard curve with a range from 5.0 to 6.6.

RESULTS

Isolation and Molecular Characterization of A. thaliana Mutant Plants Containing AHA1 and AHA2 Gene Disruptions—The *Arabidopsis* genome carries 11 similar but discrete members of the plasma membrane proton pump family (*AHA1–11*, for *A*rabidopsis H^+-ATPase isoforms 1–11). The AHAs are a subfamily of the P-type ATPase superfamily, which has 46 members in *Arabidopsis*, and the other members transport specific solutes other than protons (25). Thus, only the 11 AHA isoforms appear to catalyze the ATP-dependent active efflux of protons across the plasma membrane, resulting in a protonmotive force composed of both a membrane potential with inside negative values of −140 to −210 mV (26, 27), and a pH gradient generated by apoplastic pH 5–6 and cytoplasmic pH 7.5. There are no genes in *Arabidopsis* encoding a sodium pump, or any other known primary active transport system, suggesting that members of the AHA family satisfy all of the primary active transport requirements of this organism. Transcriptome analysis of the 11 *AHA* members based on hybridization to DNA chips or the number of expressed sequence tags reflecting mRNA abundances indicates that *AHA1* and *AHA2* are by far the most highly expressed members of this family throughout plant life (Fig. 1, *A* and *B*). In addition, when the 11 protein sequences are compared for sequence similarities via a phylogenetic tree, it is clear that AHA1 and AHA2 are the most closely related of all the members, suggesting that they arose from the recent duplication of a common ancestor (Fig. 1*A*). Expression studies with *AHA3* suggest that this enzyme plays a role in phloem transport, but because homozygous *AHA3* knock-out mutant plants are male-sterile, there is no clear genetic evidence of a critical role for AHA3 in vegetative growth (4). Genetic and expression studies with *AHA4* and *-10* suggest that they play roles in salt stress tolerance and seed coat pigmentation, but again, genetic evidence for an essential function is lacking (15, 16).

To critically test whether AHA1 or AHA2 proteins are essential, we examined the growth of various insertional mutant alleles of each gene using available T-DNA collections. All of the mutants used in this study were obtained from the Salk Collection in the Columbia ecotype, and sequence analysis of the T-DNA/plant genomic DNA junction demonstrated that the insertion occurred either within an intron (*aha1–6*, *aha1–8*, *aha2–4*, and *aha2–5*) or within an exon (*aha1–7*) (Fig. 2*A*).

To determine whether the insertional mutations resulted in growth alterations, mutants were selfed, and homozygous plants lacking wild type copies of either *AHA1* or *AHA2* genes were obtained. Growth measurements under ideal laboratory conditions revealed no growth defect in *aha1* or *aha2* mutant plants. To determine how severe the insertions were at the level of gene expression, *AHA1* and *AHA2* RNA abundances were quantified via various methods, including microarray and quantitative RT-PCR (Fig. 2). The results of these experiments demonstrated that *aha1–6* and *aha1–8* mutants carry knockdown *AHA1* alleles, and the *aha1–7* mutant appears to express a truncated *AHA1* transcript whose abundance at the post-in-

A

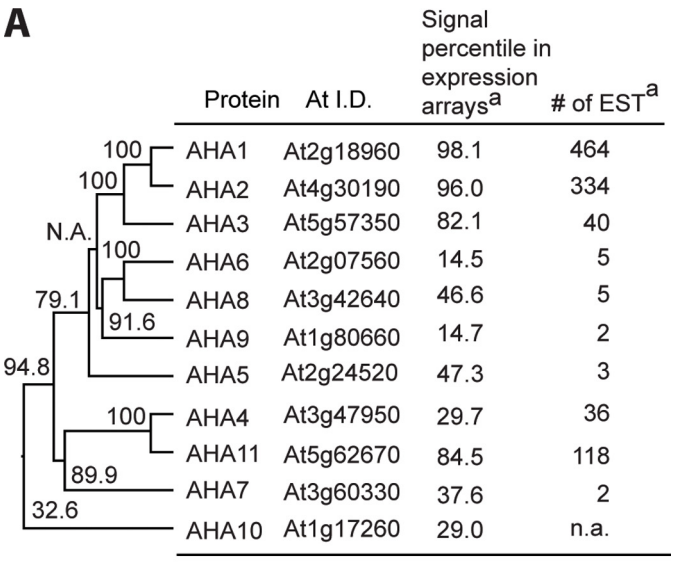

Protein	At I.D.	Signal percentile in expression arrays[a]	# of EST[a]
AHA1	At2g18960	98.1	464
AHA2	At4g30190	96.0	334
AHA3	At5g57350	82.1	40
AHA6	At2g07560	14.5	5
AHA8	At3g42640	46.6	5
AHA9	At1g80660	14.7	2
AHA5	At2g24520	47.3	3
AHA4	At3g47950	29.7	36
AHA11	At5g62670	84.5	118
AHA7	At3g60330	37.6	2
AHA10	At1g17260	29.0	n.a.

B

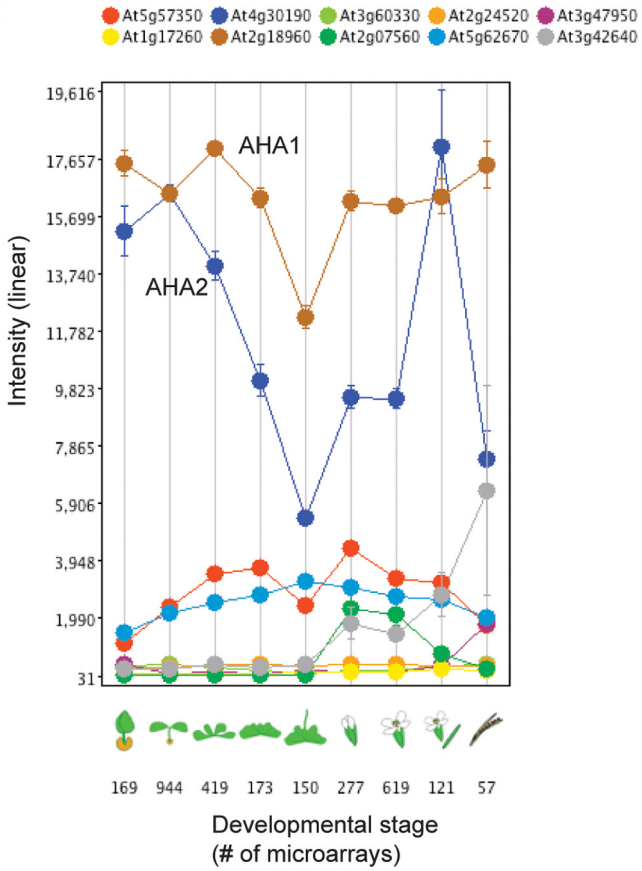

FIGURE 1. **Phylogenetic and expression analyses of 11 AHA members.** *A*, phylogenetic tree and expression level of AHA members based on microarray and expression sequence tag analyses. Protein sequences were aligned by an algorithm, ClustalV (PAM250), provided by Megalign (Lasergene, DNASTAR, Inc., Madison, WI). Bootstrap values (%) obtained by resampling 1000 times were indicated at the branches of the tree. *n.a.*, not available. [a], data were obtained on line. *B*, developmental expression study of AHA members with Genevestigator. Data were obtained on line.

sertion region was below the detection threshold. Although *aha1–7* lacks the *AHA1* full-length transcript, we were unable to determine whether its predicted protein that is truncated adjacent to amino acid 739 within the M7–M8 extracellular loop has catalytic activity. *AHA2* expression in the *aha2–4* and *aha2–5* mutants was reduced by 90–95% in both cases, compared with wild type plants. In addition, these studies demonstrated that in all of the insertional mutant plants showing reduced *AHA1* or *-2* levels, there was no compensation observed at the transcript level. In other words, reduced levels of *AHA1* or *AHA2* did not result in increased levels of any other *AHA* isoform (Fig. 2, *B* and *C*).

To determine whether compensation was occurring at the translational level, protein abundance was analyzed via mass spectrometric approaches. Plants were grown and plasma membranes were isolated from wild type, *aha1–6* and *aha2–4* mutants. After trypsinization, peptides were subjected to analysis on an ESI-LTQ-Orbitrap tandem mass spectrometer. Because AHA1 and AHA2 are very conserved at the amino acid sequence level (94.4% identity), it was essential to identify and quantify the tryptic peptides with isoform-specific peptide sequences. Two tryptic peptides, from amino acid 407 to 420 and 471 to 490, in AHA1 and AHA2 were particularly informative in this regard. As shown in Fig. 2, *D* and *E*, by quantifying the relative intensity of these peptide ions in the extracted chromatogram, we were able to determine that, consistent with the mRNA studies, the mutants have reduced levels of AHA1 or AHA2 proteins. In addition, the mass spectrometric measurements demonstrated that there were no increases in the AHA2 protein nor any other AHA isoforms in the *aha1–6* mutants and vice versa, *i.e.* there was no compensation occurring at the translational level in the *aha1–6* or *aha2–4* mutants.

It is well established that protein kinase-mediated phosphorylation of the penultimate threonine in the plasma membrane proton pump can result in a hyperactive enzyme, with increased catalytic activity (28). We thus sought a method to measure the stoichiometry of phosphorylation for AHA1 and AHA2 at this residue, to determine whether the homozygous mutant plants were compensating for the loss of one of the isoforms by an increase in the level of phosphorylation of the other, and/or of the small amount of residual ATPase remaining in the insertional mutants. For this purpose, we chose a highly sensitive and quantitative method, selected reaction monitoring, with heavy isotope synthetic peptides directed against a C-terminal tryptic fragment as follows: AHA1, $^{+}$GLDIDTAGHHYTV^{-}; AHA2, $^{+}$GLDIDTAGHYTV^{-}. Heavy isotope-labeled peptides with and without phosphorylation at AHA1 Thr-948 or AHA2 Thr-947 were synthesized and used as internal standards for absolute quantitation of the C-terminal tryptic peptide from both AHA1 and AHA2 with a triple quadrupole mass spectrometer. By inferring the abundance of AHA1 and AHA2 proteins as the sum of phosphorylated and unphosphorylated forms of the C-terminal peptides, we confirmed our earlier result of untargeted analysis with the LTQ-Orbitrap mass spectrometer that there was no compensation at the translational level observed in the *aha1–6* or *aha2–4* mutants. With the targeted analysis, however, we observed significant increases in AHA1 phosphorylation level of the residual AHA1 protein in *aha1–6* mutants (Fig. 2*F*). Similarly, AHA2 phosphorylation level of the residual AHA2 protein was increased in *aha2–4* mutant. There were also small increases in the phosphorylation of AHA1 protein in *aha2–4* mutant as

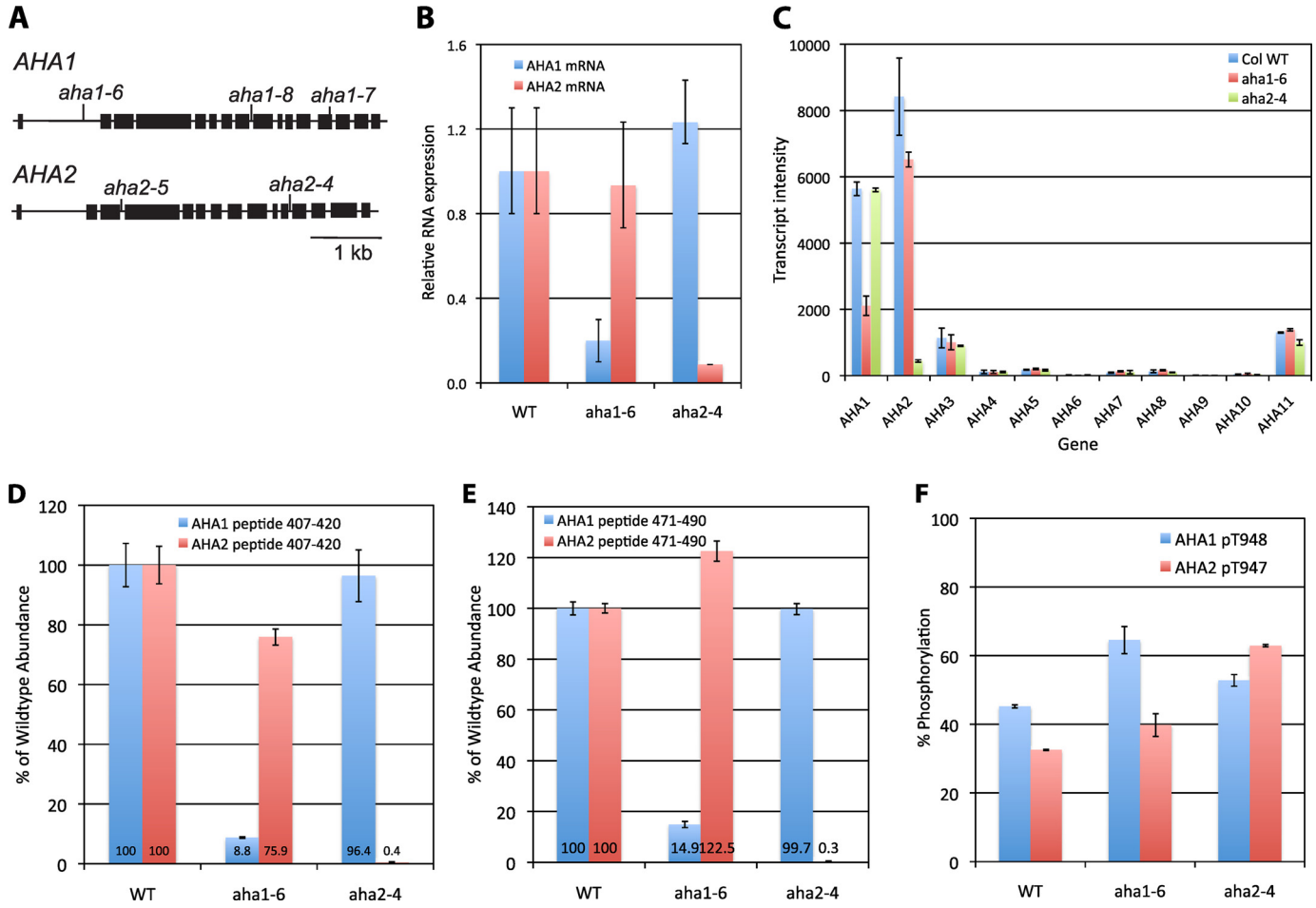

FIGURE 2. **Molecular characterization of loss-of-function mutants of AHA1 and AHA2.** *A*, description of the T-DNA insertional alleles of *AHA1* and *AHA2*. *Black boxes* represent exons. *Vertical lines* indicate the location of T-DNAs. *aha1–6*, SALK016325; *aha1–7*, SALK065288; *aha1–8*, SALK118350; *aha2–4*, SALK082786; and *aha2–5*, SALK022010. *B*, quantitative RT-PCR of *AHA1* and *AHA2* in wild type (*WT*), *aha1–6*, and *aha2–4* mutants. *C*, transcript signal intensities of the 11 AHA members in WT, *aha1–6*, and *aha2–4* mutants determined by microarray analyses. *Graph* shows mean values with S.D. *D* and *E*, AHA1 and AHA2 protein abundances in WT, *aha1–6*, and *aha2–4* plants. Isoform-specific polypeptides (the amino acid position 407–420 and 471–490) were determined by quantifying the peak areas of the peptide ions found in the total ion chromatogram of mass spectrometric analyses. Data are shown as means ± S.E. of three separate measurements. *F*, selective reaction monitoring mass spectrometry analysis for AHA1 and -2 C-terminal peptides of nonphosphorylated and phosphorylated forms. Proportion of AHA1 phosphopeptide Thr(P)-948 and AHA2 phosphopeptide Thr(P)-947 was quantified and shown ± S.D. *Col WT*, wild type plant of A. thaliana, ecotype Columbia.

well as in that of AHA2 protein in *aha1–6* mutant. Our results are consistent with an increase in kinase-mediated phosphorylation of the penultimate Thr residue behaving as a post-translational means of compensating for the loss of AHA proteins. Although the trends were clear, the errors associated with the measurements do not allow a clear estimate of the degree of compensation attained.

Simultaneous Disruption of both AHA1 and AHA2 Genes in a Single Plant Is Lethal—To obtain a single plant containing both *AHA1* and *AHA2* gene disruptions, various *aha1* and *aha2* mutants were crossed, and seeds resulting from the dihybrid plants were selfed. Progeny from this population was then examined to determine whether any plants lacking both *AHA1* and *2* wild type alleles could be obtained. As shown in Table 2, with three different pairs of mutants crossed (*i.e. aha1–6* and *aha2–4*; *aha1–7* and *aha2–5*; and *aha1–8* and *aha2–5*), a homozygous double mutant was never recovered in the progeny, suggesting that the double mutation was lethal at some point during gametogenesis or embryogenesis.

TABLE 2

Plant lines segregating *aha1* and *aha2* mutant alleles failed to produce homozygous double mutants

The genotypes of progeny from $AHA1^{+/-}AHA2^{+/-}$ mutants were determined using a PCR-based method.

Parent genotype	No. of progeny genotyped	No. of homozygous double mutants observed	No. of homozygous double mutants expected
AHA1/aha1–6 AHA2/aha2–4	243	0	15
AHA1/aha1–7 AHA2/aha2–5	52	0	3
AHA1/aha1–8 AHA2/aha2–5	55	0	3

To identify the developmental stage first affected by the double mutant condition, we analyzed the segregation pattern of the *aha1–6* allele from plants homozygous for the *aha2–4* mutations and heterozygous for the *aha1–6* mutation. The observed ratios of progeny allele frequencies were subjected to the χ^2 test to examine whether our hypothesis for embryonic lethality in the homozygous double mutants is statistically supported. The results indicate that lethality is likely to occur dur-

TABLE 3

Progeny of *AHA1/aha1–6 aha2–4/aha2–4* and *aha1–6/aha1–6 AHA2/aha2–4* parents

The genotypes of F3 progeny were determined by PCR. Ob. indicates the number of individuals observed; Ex. 1 indicates the expected number based on Mendelian inheritance. Ex. 2 indicates the expected number when the homozygous double mutant plants are not viable due to lethality during embryogenesis. Ex. 3 indicates the expected number when the double mutant plants are not viable due to lethality during gametogenesis. χ^2 test was used to determine the probability of which the deviation of the observed value from the expected value was due to chance.

Parent genotype	Progeny genotype	Ob.	Ex. 1	Ex. 2	Ex. 3
AHA1/aha1–6 aha2–4/aha2–4	*AHA1/AHA1 aha2–4/aha2–4*	28	20.5	27.3	41
	AHA1/aha1–6 aha2–4/aha2–4	54	41	54.7	41
	aha1–6/aha1–6 aha2–4/aha2–4	0	20.5	0	0
			$p < 0.001$	$p > 0.95$	$p < 0.01$
aha1–6/aha1–6 AHA2/aha2–4	*aha1–6/aha1–6 AHA2/AHA2*	13	10.5	14	21
	aha1–6/aha1–6 AHA2/aha2–4	29	21	28	21
	aha1–6/aha1–6 aha2–4/aha2–4	0	10.5	0	0
			$p < 0.001$	$p > 0.95$	$p < 0.05$

TABLE 4

Gametophytic transmission of *aha1–6* and *aha2–4* alleles determined by reciprocal crosses

Two sets of reciprocal crosses were performed to examine the transmission of *aha1–6 aha2–4* double mutations through the male or female gametes. The mutant parents are *AHA1/aha1–6 aha2–4/aha2–4* or *aha1–6/aha1–6 AHA2/aha2–4,* and the other parent is wild type (*AHA1/AHA1 AHA2/AHA2*).

Female parent genotype	Male parent genotype	Progeny genotype	
		AHA1/AHA1 AHA2/aha2–4	*AHA1/aha1–6 AHA2/aha2–4*
AHA1/aha1–6 aha2–4/aha2–4	*AHA1/AHA1 AHA2/AHA2*	24	29
AHA1/AHA1 AHA2/AHA2	*AHA1/aha1–6 aha2–4/aha2–4*	18	14
		AHA1/aha1–6 AHA2/AHA2	*AHA1/aha1–6 AHA2/aha2–4*
aha1–6/aha1–6 AHA2/aha2–4	*AHA1/AHA1 AHA2/AHA2*	14	14
AHA1/AHA1 AHA2/AHA2	*aha1–6/aha1–6 AHA2/aha2–4*	13	15

ing embryo development rather than during gamete development (Table 3). A similar result was obtained in reciprocal experiments testing the *aha2–4* allele segregation pattern from double mutants homozygous for the *aha1–6* mutation and heterozygous for the *aha2–4* mutation. We also analyzed the transmission efficiencies of the insertional mutant alleles through the male and female gametes. We performed two sets of reciprocal crosses between wild type plants and plants heterozygous for one *AHA* insertion allele and homozygous for the other. In the subsequent progeny, we observed normal transmission efficiencies of the *aha1–6* and *aha2–4* mutations through both pollen and ovule, indicating that the double mutations do not affect female or male gametogenesis (Table 4).

In the course of our experiments, we observed aborted developing seeds within the siliques of self-pollinated flowers from the double mutant plants that carry only one wild type copy of either *AHA1* or *AHA2.* The aborted seeds were randomly distributed and accounted for approximately one-quarter of the total number of seeds within the silique (Fig. 3, *A–D*). Wild type plants or either *aha1–6* or *aha2–4* single mutants grown in the same environment rarely showed aborted seeds within their siliques. To investigate early seed abortion in putative homozygous double mutants, we microscopically examined thin tissue sections of developing seeds from self-pollinated plants that are homozygous mutants at the *AHA1* locus and heterozygous mutants at the *AHA2* locus. Whereas ~75% of the seeds within the analyzed siliques contained embryos at the globular heart transition stage, the remaining 25% contained embryos arrested at the pre-globular stage (Fig. 3, *E–I*). We hypothesized that these arrested embryos are the nonviable homozygous double mutants. The same results were observed with reciprocal sets of double mutants.

To test whether there is a causal link between the homozygous double mutant genotype and the lethal phenotype, we carried out molecular complementation. A 10-kb genomic DNA fragment, including the *AHA1* gene and the entire regulatory region, was introduced into double mutant plants that lack wild type copies of the *AHA1* gene. A total of 184 independently transformed plants (T1) were recovered and further screened. We obtained 11 homozygous double mutant plants carrying wild type *AHA1* transgenes among the T1 population (Table 5). Genotyping of the T2 progeny resulting from self-fertilization of the rescued lines confirmed the existence of plants homozygous for the *aha1–6* and *aha2–4* alleles that are viable due to the presence of the *AHA1* transgene. Similar results were obtained when we transformed double mutant plants that lack wild type copies of the *AHA2* gene with a genomic DNA fragment, including the *AHA2* gene and regulatory region (Table 5).

Our successful complementation of the double mutants with either *AHA1* or *AHA2* transgenes provides us a system for further investigating the structure-function relationship of AHA proteins. The double mutant plants whose endogenous *AHA1* and *AHA2* genes are replaced with tagged transgenes would be useful for analyzing AHA protein localization and post-translational modifications. To explore a potential site for inserting a tag within AHA2 protein, we created a point mutation in this transgene. To avoid generating mutations within the activity regulatory domains at the N- or C-terminal ends (29), the M9–M10 extracellular loop was chosen as a target site. A mutation was created to introduce a restriction enzyme (XbaI) site for cloning purposes at the amino acid Trp-807 position, which converts this residue into a dimer, Leu-Glu (W807L/W807E mutation). This *AHA2* transgene carrying the W807L/W807E mutation successfully rescued the embryo lethality of the homozygous double mutants (Table 5), and the rescued plants appeared to be normal, suggesting this single amino acid insertion at the loop does not influence the AHA2 catalytic activity. Next, we transformed the

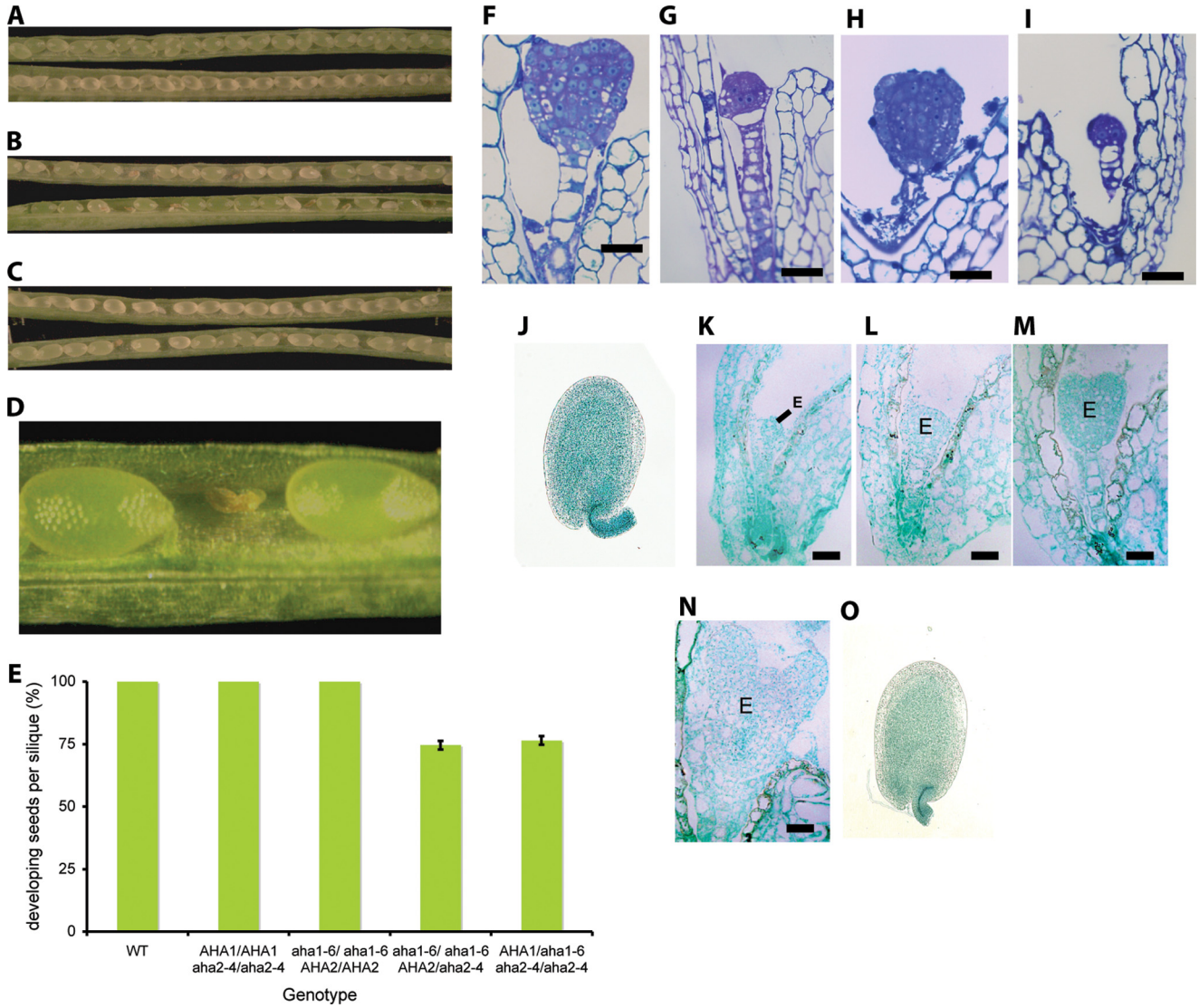

FIGURE 3. **Seed developments in the double mutants and *AHA1* and *AHA2* promoter activity.** *A*, phenotype of seed development in WT viewed under a stereomicroscope. *B*, immature siliques of *aha1–6/aha1–6 AHA2/aha2–4* plants containing empty spaces. *C*, immature siliques of *AHA1/aha1–6 aha2–4/aha2–4* plants containing empty spaces. *D*, magnified view of an aborted seed in a silique of *aha1–6/aha1–6 AHA2/aha2–4* plant. *E*, percentage of developing seeds from the double mutants compared with WT or the *AHA* single mutant plants. *Bars* indicate S.E. *F*, normal growing embryo from self-pollinated *aha1–6/aha1–6 AHA2/aha2–4* plants. *G*, arrested embryos from the same silique as in *F*. *H*, normal growing embryo from self-pollinated *AHA1/aha1–6 aha2–4/aha2–4* plants. *I*, arrested embryos from the same silique as in *H*. *Scale bar*, 20 μm. *J–N*, GUS staining in embryos for *AHA1* promoter activity. *J*, developing seed; *K*, 8-cell stage; *L*, early globular stage; *M*, late globular stage; *N*, heart stage. *Scale bar*, 20 μm. *O*, GUS staining in developing seed for *AHA2* promoter activity. *Scale bar*, 10 μm. *E*; embryo.

double mutants with the *AHA2* transgene that carries green fluorescent protein as an in-frame insertion at this Trp-807 position to produce an ~125-kDa AHA2-GFP fusion pump protein; however, no rescued homozygous double mutants were recovered from the transgenic population, suggesting that this modified AHA2(W807GFP) transgene did not complement the embryo lethality and that the AHA2 protein conformation was unlikely to be able to tolerate a large polypeptide insertion at this extracellular location.

The fact that the *aha1 aha2* homozygous double mutant embryos failed to develop properly indicates that *AHA1* and *AHA2* are transcriptionally active during embryogenesis. To test this prediction, we studied *AHA1* and *AHA2* promoter activities using a GUS reporter gene assay. Plants carrying a 3.4-kb *AHA1* promoter or a 3.2-kb *AHA2* promoter region and the first exon fused with GUS were generated and assayed for GUS activity. Histochemical staining for GUS activity indicates that the *AHA1* promoter is active on the surface of developing seeds and from 8- to 16-cell stages to the heart stage of embryo development (Fig. 3, *J–N*). In contrast, GUS staining for the *AHA2* promoter activity was observed much lower than the *AHA1* promoter on the surface of developing seeds (Fig. 3*O*) and was detected up to the early globular stage of embryo development.

Growth of Wild Type and AHA Mutants under a Large Number of Environmental Challenges—The fact that the homozygous double mutants are embryo-lethal supports the hypothesis that, collectively, the two genes perform an essential function. Their roles in vegetative growth, however, remain to be determined. To investigate the functions of *AHA1* and *-2*

TABLE 5

Molecular complementation of *aha1–6/aha1–6;aha2–4/aha2–4* plants with wild type or modified transgenes of *AHA1* or *AHA2*

Transgene	% of rescued plants in T1 population[a]	% of rescued plants[b] in T2 population
Wild type *AHA1* genomic clone[c]	5.98% ($n = 184$)	21.4% ($n = 42$) 16.7% ($n = 42$)
Wild type *AHA2* genomic clone[d]	5.56% ($n = 90$)	15.4% ($n = 39$) 23.3% ($n = 30$)
AHA2(W807LE)[e]	4.3% ($n = 23$)	20.0% ($n = 30$) 15.3% ($n = 32$)
AHA2(W807GFP)[f]	0% ($n = 82$)	0% ($n = 30$) 0% ($n = 30$)

[a] Numbers in parentheses indicate total numbers of transformed plants that were PCR-genotyped.
[b] T2 progeny of two independently transformed lines from *AHA1/aha1–6;aha2–4/aha2–4* or *aha1–6/aha1–6;AHA2/aha2–4* plants carrying transgenes were genotyped to identify rescued plants.
[c] *aha1–6/aha1–6;AHA2/aha2–4* plants were transformed with wild type *AHA1* gene.
[d] *AHA1/aha1–6;aha2–4/aha2–4* plants were transformed with wild type *AHA2* gene.
[e] *AHA2* genomic clone with a mutation of Trp-807 to Leu-Glu to create an XbaI restriction enzyme site.
[f] *AHA2* genomic clone with a translational fusion to green fluorescent protein that is inserted at the Trp-807.

during vegetative growth, we grew *aha1* and *aha2* homozygous single mutants under >100 different environmental conditions (supplemental material). Although there are many different growth/developmental analyses one could make, we chose to measure root length because this can be done quantitatively under a large number of conditions. The list of environmental challenges was chosen based on known or suspected functions of the pump. For example, a role of the pump in auxin-mediated cell elongation has long been considered important for mechanistic models of plant cell elongation. Thus, studies were performed with *aha1* and *aha2* mutant plants grown in the presence of various concentrations of added auxin and other hormones. Surprisingly, in root elongation assays, only a few out of over 100 conditions elicited a difference between wild type and mutant plants. Notably, none of the known phytohormones (gibberellic acid, abscisic acid, kinetin, ethylene (1-aminocyclopropane-1-carboxylic acid), and iodole-3-acetic acid) nor plant growth regulators (brassinolide and jasmonate) produced a difference in root growth among the three genotypes. Of all the many changes to the medium, the only two in which the mutants fared worse than wild type were those expected to alter the protonmotive force across the plasma membrane (a high external potassium concentration and high external pH) (Fig. 4*A*). As shown in Fig. 4, *B* and *C*, the effect of potassium was only observed at concentrations ≥50 mM and was specific for potassium because neither sodium chloride nor sorbitol produced a differential effect on root growth of the two mutants. It is well known that high concentrations of potassium cause a decrease in membrane potential (26), which is not elicited by high concentrations of less permeable cations like sodium or with neutral solutes like sorbitol, which also eliminates an effect of osmotic response because all three compounds (potassium, sodium and sorbitol) are capable of causing osmotic stresses. Similarly, it is likely that at high external pH, the protonmotive force is compromised because there is a 100-fold decrease in proton concentration going from pH 6.0 to 8.0 in the external medium. It is likely that both the potassium-induced decrease in membrane potential and the alkaline external pH exerted stresses on the ability of the proton pump to maintain a sufficient protonmotive force to support growth, which could not be overcome in the AHA-impaired mutants. In all cases, the phenotypic differences are more pronounced in the *aha2* mutants, which is consistent with the greater impairment in pump mRNA and protein levels found in these mutants, and in the greater importance that this isoform is likely to have in roots, given its pattern of expression (30).

It is interesting to note that the only other environmental conditions that elicited a difference between genotypes were the additions of a variety of toxic cations. In all of these cases, there was a marked advantage in growth in the mutants, compared with the wild type. This phenomenon was observed with aminoglucoside antibiotics, including hygromycin and gentamicin, and with alkali metal ions, including lithium and cesium, and is consistent with the reduced uptake of a toxic compound in roots of plants containing reduced protonmotive force (Fig. 4, *D–G*). Consistent with this interpretation, we demonstrated that the hygromycin effect could be reduced by the presence of 50 mM potassium chloride but not 50 mM sodium chloride (Fig. 4*H*). In other words, when the overall membrane potential was reduced by potassium, so that little hygromycin was entering root cells, there was no difference among the three genotypes. In the absence of high potassium, however, when the membrane potential was driving hygromycin transport into root cells, the *aha2* mutants showed less sensitivity to the toxic cation. A similar observation has been made in yeast mutants with impaired PMA1 activity. In fact, hygromycin-insensitive mutants were the first plasma membrane proton pump mutants to be found in early work with *Saccharomyces cerevisiae* (31).

Measurements of AHA1 and AHA2 Pump Activity—The above experiments demonstrate the growth consequences caused by reduced proton pump activity in the *aha2* and *aha1* mutants, although there were no such apparent consequences when the plants were grown under ideal laboratory conditions without environmental challenges such as high potassium or high external pH. In addition, although we were unable to ascertain to what extent the increased phosphorylation status of the penultimate threonine could compensate for loss of an isoform, it is possible that this kinase-mediated mechanism allows plant tissues to maintain a wild type level of pump activity in each of the single mutants. Thus, to provide a more direct answer to the question of whether the mutant plants contain reduced catalytic activity, we measured the bathing medium pH during root growth. We used an indicator dye, fluorescein, to measure and compare pH changes in root rhizosphere from the wild type *versus* mutant plants. This assay has been used previously in higher plants as a measure of root surface pH (32). As shown in Fig. 5, we observed that the *aha2* mutant plant was clearly impaired in proton-secreting activities, compared with wild type, and that the *aha1* mutants appeared normal compared with wild type. These results reinforce our previous demonstrations that the *aha2* mutants are more severe in their root growth defects compared with *aha1* and, more importantly, are a direct demonstration that pump activity is impaired in *aha2* mutants even under ideal laboratory conditions.

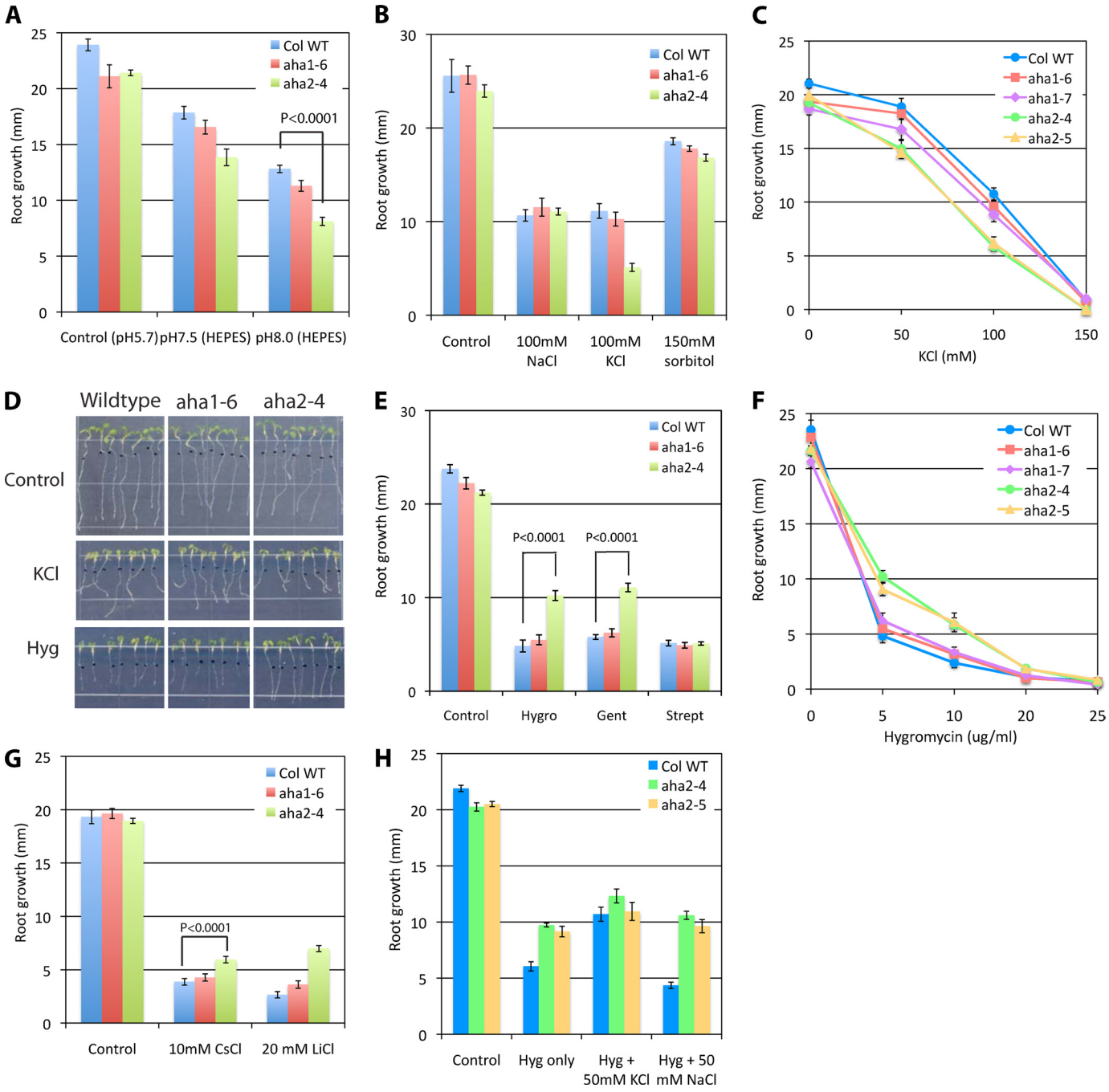

FIGURE 4. **Root growth phenotypes of *aha1* and *aha2* mutants in response to treatments that perturb the protonmotive force.** *A*, high pH sensitivity of root growth in *aha2* mutant. *B*, high potassium sensitivity of root growth in *aha2* mutant. *C*, dose-response effects of potassium on *aha1* and *aha2* root growth. *D*, images of root growth on control, KCl, and hygromycin media. *E*, effects of aminoglucoside antibiotics on *aha2* root growth. *Hygro*, 5 μg/ml hygromycin; *Gent*, 10 μg/ml gentamicin; *Strept*, 100 μg/ml streptomycin. *F*, dose-response effects of hygromycin B on *aha1* and *aha2* root growth. *G*, cesium and lithium tolerance in *aha2* mutant. *H*, suppression of hygromycin inhibitory effect by potassium. *Col WT*, wild type plant of A. thaliana, ecotype Columbia.

DISCUSSION

In this study, we characterize the function of the two most highly expressed members, *AHA1* and *AHA2*, from the plasma membrane proton pump gene family, using *Arabidopsis* loss-of-function mutant plants. Our experiments demonstrate that although there is little consequence of impairing the function of either AHA1 or AHA2 in *Arabidopsis* plants grown under ideal conditions, the loss of both genes is absolutely lethal, blocking embryogenesis at an early stage of development. The successful complementation of the embryo lethality with either *AHA1* or *AHA2* transgenes proves that a single copy of either gene is equally sufficient to maintain the protonmotive force in these plants. Unlike work in animals with the Na^+/K^+-ATPase where there is a specific inhibitor available (33), there are no selective inhibitors for the plasma membrane proton pump. Thus, the loss-of-function mutants characterized here represent useful tools to investigate *in planta* roles of the proton pump. Consistent with the genetic experiments performed in other

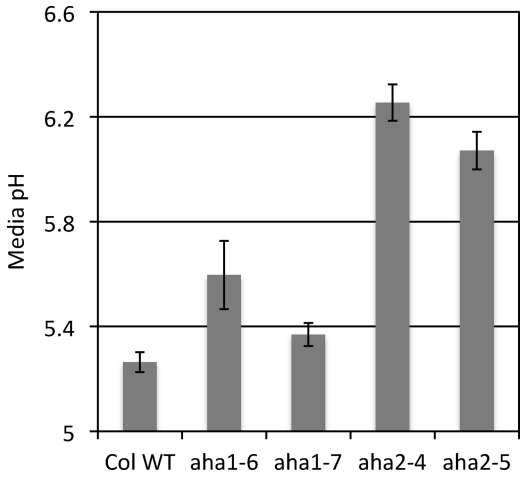

FIGURE 5. **Proton-secreting activity in roots of wild type and *aha1* and *aha2* mutants.** Representative extracellular pH assay reflecting plasma membrane proton pump activity. pH of bathing media was quantified with fluorescein dye. $n = 7$; *error bars* indicate S.E. *Col WT*, wild type plant of A. thaliana, ecotype Columbia.

model organisms, our results demonstrate the prerequisite of the plasma membrane electrochemical gradient for life. Whereas a single gene deletion is sufficient to reveal the essential role of the primary active transport pumps in other organisms (Table 1), the necessity of deleting the two pump genes in *Arabidopsis* may indicate that this redundancy is a useful part of evolutionary adaptation of the higher plants as sessile multicellular organisms.

We further show that although plants harboring *aha1* or *aha2* single gene mutations do not compensate for the loss by increasing the expression of the other AHA members at the RNA or protein levels, there is a post-translational compensatory measure. Phosphorylation of the penultimate threonine in the remaining AHA1 protein in the *aha1* mutant or that in remaining AHA2 proteins in *aha2* mutant is significantly upregulated. Phosphorylative compensation for the loss of one isoform in either *aha1* or *aha2* mutants, however, was observed only to a small extent. Despite this increase in the level of regulatory phosphorylation, *aha2* mutants contain reduced levels of overall catalytic activity in their roots, as demonstrated directly by measurements of proton secretion and indirectly by impaired reaction to conditions that reduce the protonmotive force and place strain on the ability of the cell to maintain a sufficient driving force for transport-related growth requirements. The growth advantage that the *aha2* mutants show over wild type in the presence of toxic cations like hygromycin, cesium, and lithium is also a clear indicator that the protonmotive force is impaired. The differential phenotypic responses in the *aha1* and *aha2* mutants to a variety of stresses are likely due to isoform-specific expression in root cells, because *AHA2* is more highly expressed in the root epidermal cells compared with *AHA1*.

Finally, we report on a method using heavy isotope-labeled synthetic peptides corresponding to the phosphorylated and nonphosphorylated versions of the C-terminal tryptic fragment of the AHAs, in which selected reaction monitoring with a triple quadrupole mass spectrometer is used to measure the stoichiometry of phosphorylation of the pump. This method is amenable to high throughput use under a range of conditions and, together with transgene-mediated genetic complementation studies using the double mutant lines, will provide a new approach for understanding the *in planta* role played by the plasma membrane proton pump in higher plants.

Acknowledgments—We gratefully acknowledge Ed Huttlin and Gary Case for peptide designing and synthesis; Patrick Krysan for assistance with microscopy; David C. Nelson, Melissa LeBlanc, and Jeffrey Harper for constructive discussions; Fernando I. Rodríguez and Angie Bewell for technical assistance; and Wayne Davis and Sandra Splinter BonDurant for assistance with the microarray experiment.

REFERENCES

1. Lingrel, J. B., Williams, M. T., Vorhees, C. V., and Moseley, A. E. (2007) *J. Bioenerg. Biomembr.* **39,** 385–389
2. de Carvalho Aguiar, P., Sweadner, K. J., Penniston, J. T., Zaremba, J., Liu, L., Caton, M., Linazasoro, G., Borg, M., Tijssen, M. A., Bressman, S. B., Dobyns, W. B., Brashear, A., and Ozelius, L. J. (2004) *Neuron* **43,** 169–175
3. Serrano, R., Kielland-Brandt, M. C., and Fink, G. R. (1986) *Nature* **319,** 689–693
4. Robertson, W. R., Clark, K., Young, J. C., and Sussman, M. R. (2004) *Genetics* **168,** 1677–1687
5. Davis, M. W., Somerville, D., Lee, R. Y., Lockery, S., Avery, L., and Fambrough, D. M. (1995) *J. Neurosci.* **15,** 8408–8418
6. Feng, Y., Huynh, L., Takeyasu, K., and Fambrough, D. M. (1997) *Genes Funct.* **1,** 99–117
7. Palladino, M. J., Bower, J. E., Kreber, R., and Ganetzky, B. (2003) *J. Neurosci.* **23,** 1276–1286
8. Ellertsdottir, E., Ganz, J., Dürr, K., Loges, N., Biemar, F., Seifert, F., Ettl, A. K., Kramer-Zucker, A. K., Nitschke, R., and Driever, W. (2006) *Dev. Dyn.* **235,** 1794–1808
9. Shu, X., Cheng, K., Patel, N., Chen, F., Joseph, E., Tsai, H. J., and Chen, J. N. (2003) *Development.* **130,** 6165–6173
10. James, P. F., Grupp, I. L., Grupp, G., Woo, A. L., Askew, G. R., Croyle, M. L., Walsh, R. A., and Lingrel, J. B. (1999) *Mol. Cell* **3,** 555–563
11. Moseley, A. E., Williams, M. T., Schaefer, T. L., Bohanan, C. S., Neumann, J. C., Behbehani, M. M., Vorhees, C. V., and Lingrel, J. B. (2007) *J. Neurosci.* **27,** 616–626
12. Merlot, S., Leonhardt, N., Fenzi, F., Valon, C., Costa, M., Piette, L., Vavasseur, A., Genty, B., Boivin, K., Müller, A., Giraudat, J., and Leung, J. (2007) *EMBO J.* **26,** 3216–3226
13. Zhao, R., Dielen, V., Kinet, J. M., and Boutry, M. (2000) *Plant Cell* **12,** 535–546
14. Gévaudant, F., Duby, G., von Stedingk, E., Zhao, R., Morsomme, P., and Boutry, M. (2007) *Plant Physiol.* **144,** 1763–1776
15. Vitart, V., Baxter, I., Doerner, P., and Harper, J. F. (2001) *Plant J.* **27,** 191–201
16. Baxter, I. R., Young, J. C., Armstrong, G., Foster, N., Bogenschutz, N., Cordova, T., Peer, W. A., Hazen, S. P., Murphy, A. S., and Harper, J. F. (2005) *Proc. Natl. Acad. Sci. U.S.A.* **102,** 2649–2654
17. Santi, S., and Schmidt, W. (2009) *New Phytol.* **183,** 1072–1084
18. Alonso, J. M., Stepanova, A. N., Leisse, T. J., Kim, C. J., Chen, H., Shinn, P., Stevenson, D. K., Zimmerman, J., Barajas, P., Cheuk, R., Gadrinab, C., Heller, C., Jeske, A., Koesema, E., Meyers, C. C., Parker, H., Prednis, L., Ansari, Y., Choy, N., Deen, H., Geralt, M., Hazari, N., Hom, E., Karnes, M., Mulholland, C., Ndubaku, R., Schmidt, I., Guzman, P., Aguilar-Henonin, L., Schmid, M., Weigel, D., Carter, D. E., Marchand, T., Risseeuw, E., Brogden, D., Zeko, A., Crosby, W. L., Berry, C. C., and Ecker, J. R. (2003) *Science* **301,** 653–657
19. Krysan, P. J., Young, J. C., Tax, F., and Sussman, M. R. (1996) *Proc. Natl. Acad. Sci. U.S.A.* **93,** 8145–8150
20. Bolstad, B. M., Irizarry, R. A., Astrand, M., and Speed, T. P. (2003) *Bioinformatics* **19,** 185–193
21. Nelson, C. J., Hegeman, A. D., Harms, A. C., and Sussman, M. R. (2006)

Mol. Cell. Proteomics **5,** 1382–1395
22. Larsson, C., Sommarin, M., and Widell, S. (1994) *Methods Enzymol.* **228,** 451–469
23. Wessel, D., and Flügge, U. I. (1984) *Anal. Biochem.* **138,** 141–143
24. Clough, S. J., and Bent, A. F. (1998) *Plant J.* **16,** 735–743
25. Baxter, I., Tchieu, J., Sussman, M. R., Boutry, M., Palmgren, M. G., Gribskov, M., Harper, J. F., and Axelsen, K. B. (2003) *Plant Physiol.* **132,** 618–628
26. Hirsch, R. E., Lewis, B. D., Spalding, E. P., and Sussman, M. R. (1998) *Science* **280,** 918–921
27. Fuglsang, A. T., Guo, Y., Cuin, T. A., Qiu, Q., Song, C., Kristiansen, K. A., Bych, K., Schulz, A., Shabala, S., Schumaker, K. S., Palmgren, M. G., and Zhu, J. K. (2007) *Plant Cell* **19,** 1617–1634
28. Lecchi, S., Nelson, C. J., Allen, K. E., Swaney, D. L., Thompson, K. L., Coon, J. J., Sussman, M. R., and Slayman, C. W. (2007) *J. Biol. Chem.* **282,** 35471–35481
29. Ekberg, K., Palmgren, M. G., Veierskov, B., and Buch-Pedersen, M. J. (2010) *J. Biol. Chem.* **285,** 7344–7350
30. Harper, J. F., Manney, L., DeWitt, N. D., Yoo, M. H., and Sussman, M. R. (1990) *J. Biol. Chem.* **265,** 13601–13608
31. McCusker, J. H., Perlin, D. S., and Haber, J. E. (1987) *Mol. Cell. Biol.* **7,** 4082–4088
32. Monshausen, G. B., Bibikova, T. N., Messerli, M. A., Shi, C., and Gilroy, S. (2007) *Proc. Natl. Acad. Sci. U.S.A.* **104,** 20996–21001
33. Yatime, L., Buch-Pedersen, M. J., Musgaard, M., Morth, J. P., Lund Winther, A. M., Pedersen, B. P., Olesen, C., Andersen, J. P., Vilsen, B., Schiøtt, B., Palmgren, M. G., Møller, J. V., Nissen, P., and Fedosova, N. (2009) *Biochim. Biophys. Acta* **1787,** 207–220